Study of toroidal current effect on rotational transform profile by MHD activity measurement in Heliotron J

G. Motojima, S. Yamamoto[a], H. Okada[b], S. Sakakibara[c], K. Y. Watanabe[c], K. Nagasaki[b], Y. Suzuki[c], T. Mizuuchi[b] , S. Kobayashi[b], B. D. Blackwell[d], Y. Nakamura, K. Kondo, K. Hanatani[b], H. Arimoto, S. Watanabe and F. Sano[b]

Graduate School of Energy Science, Kyoto University, Gokasho, Uji 611-0011, Japan
[a]Kyoto University Pioneering Research Unit for Next Generation, Gokasho, Uji 611-0011, Japan
[b]Institute of Advanced Energy, Kyoto University, Gokasho, Uji 611-0011, Japan
[c]National Institute for Fusion Science, 322-6 Oroshi-cho, Toki 509-5292, Japan
[d]Plasma Research Laboratory, Research School of Physical Sciences and Engineering, The Australian National University, Canberra, Australia

Effect of toroidal current on rotational transform has been investigated in Heliotron J by measuring magnetohydrodynamic (MHD) activities at two configurations with rotational transform ($\iota/2\pi$) close to 0.5. The resonant mode has been observed in ECH + co-NBI plasma in the configuration with $\iota/2\pi = 0.48$ at $\rho = 0.7$. This result shows that the rotational transform is probably increased due to the toroidal current. The location of the rational surface is determined at $\rho = 0.8$-0.9 by soft X-ray (SX) fluctuations related to the MHD mode. Equilibrium calculation considering the toroidal current shows that the increase of the rotational transform by the toroidal current is consistent with experimental results. The resonant mode structure has been investigated also in ECH + counter-NBI plasma at $\iota/2\pi = 0.50$ configuration, and the location of the rational surface determined by SX signals is not significantly changed compared to vacuum condition, suggesting that the change in the rotational transform profile by the toroidal current is weak due to the balance between bootstrap current and counter-flowing NB current.

Keywords: Bootstrap current, NB current, MHD instability, magnetic fluctuation, Heliotron J

1. Introduction

Suppression of magnetohydrodynamic (MHD) instability is one of the key issues for realization of high performance plasma. In helical plasmas, stabilization of pressure-driven modes such as ideal and/or resistive interchange modes is a critical issue for high-β plasma. Heliotron J is a low magnetic shear helical-axis heliotron device with a magnetic well by which, it is considered that MHD instability is expected to be avoided or stabilized [1]. However, MHD instabilities have been experimentally observed in electron cyclotron heating (ECH) and/or neutral beam injection (NBI) heated plasmas of Heliotron J [2]. The m/n = 2/1 MHD instability exhibiting intense magnetic fluctuations and low frequency (f < 10 kHz) has been observed in the plasmas with the rotational transform close to 0.5, where m and n are the poloidal and toroidal mode numbers, respectively. The equilibrium configuration is changed by a toroidal current and a plasma pressure, and a low order resonant rational surface can appear in the plasma. Toroidal currents such as bootstrap current, electron cyclotron (EC) current and neutral beam (NB) current have been examined in Heliotron J [3,4]. They can modify MHD equilibrium and stability due to the change in rotational transform ($\iota/2\pi$) profile. The effects of the toroidal current on MHD modes have been investigated in CHS [5] and W7-AS [6]. Recent experiment also indicates that the modification of rotational transform by the toroidal current may induce a spontaneous transition in Heliotron J [7]. The objective of this paper is to study the effect of toroidal current on the rotational transform by measuring MHD activities in Heliotron J.

author's e-mail:gen@center.iae.kyoto-u.ac.jp

2. Experimental setup

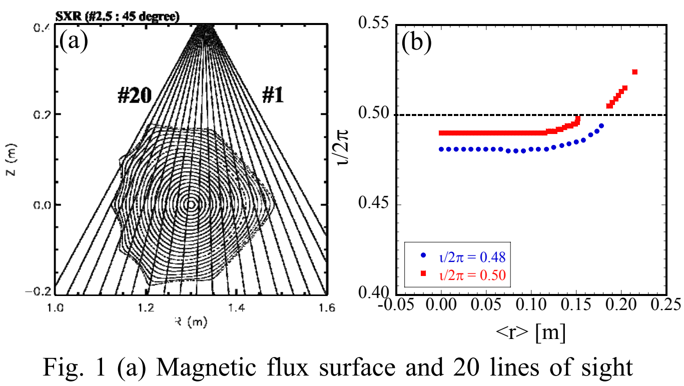

Fig. 1 (a) Magnetic flux surface and 20 lines of sight in SX array are shown. Radial profiles of rotational transform in vacuum condition are shown in (b).

Heliotron J is a medium-sized plasma experimental device. The device parameters are as follows; its plasma major radius R is 1.2 m, its averaged minor radius a is 0.1-0.2 m, its rotational transform $\iota/2\pi$ is 0.3-0.8, and its maximum magnetic field strength on the magnetic axis, B_0 is 1.5 T. The coil system is composed of an $L = 1$, $M = 4$ helical coil, two types of toroidal coils A and B, and three pairs of vertical coils. Here, L is the pole number of the helical coil and M is the pitch number of the field along the toroidal direction. A wide variety of magnetic configurations can be produced on the Heliotron J by varying the current ratios in various coils. In this study, two configurations with the rotational transform close to 0.5 were selected, namely, $\iota/2\pi = 0.48$ and 0.50 at $\rho = 0.7$ under vacuum condition while keeping magnetic field components almost constant. In Fig. 1(a), the poloidal cross-section for the $\iota/2\pi = 0.48$ configuration is shown. Figure 1(b) shows the rotational transform profiles in the vacuum condition. In this experimental condition, NB was injected to the ECH plasma (ECH+NBI plasma). Here, NB was injected to co-direction and counter-direction for negative (counter-clockwise) magnetic field and for positive (clockwise) magnetic field, respectively. The total toroidal current is measured by Rogowski coils wound on the inner wall of the poloidal cross-sections at two different toroidal angles. In order to determine the geometric structure of magnetic fluctuations accurately, 4 mirnov coils are installed in the toroidal direction and 14 mirnov coils are set poloidally on one poloidal cross section. The magnetic probes have the frequency response of up to 500 kHz. A soft X-ray (SX) diode has 20 vertical viewing chords. Figure 1(a) also shows lines of sight of the SX diode.

3. Experimental results

3.1 Separation of bootstrap current and NB current

In ECH + NBI plasmas, the toroidal current is composed of the bootstrap current and the NB current. These currents can be evaluated by comparing the experimental results obtained for positive and negative magnetic fields using the following equations, since the flow direction of the bootstrap current, which depends on $\mathbf{B}\times\nabla B$ drift, is reversed by reversing the magnetic field, while that of the NB current associated with the injected direction is not. Under the experimental conditions discussed in this paper, the effect of the EC current is weak.

$$I_{BS} = \frac{I_{\mathrm{p}}^{\mathrm{cw}} - I_{\mathrm{p}}^{\mathrm{ccw}}}{2} ,$$

$$I_{NB} = \frac{I_{\mathrm{p}}^{\mathrm{cw}} + I_{\mathrm{p}}^{\mathrm{ccw}}}{2} ,$$

where $I_{\mathrm{p}}^{\mathrm{cw}}$ and $I_{\mathrm{p}}^{\mathrm{ccw}}$ are the toroidal currents in the positive and negative magnetic field experiments, respectively. Here, we have assumed that each toroidal current component of positive magnetic field is similar to that of negative magnetic field. We confirmed the stored energy between positive and negative magnetic field was almost identical. However, we should note that absorption rate of NB is affected by the direction of magnetic field due to the change in loss rate of high energy ions. Figure 2 shows the bootstrap current and the NB current roughly evaluated. The bootstrap current is 1.5 ± 0.2 kA at $\iota/2\pi = 0.48$ case and 1.8 ± 0.3 kA at $\iota/2\pi = 0.50$ case. While, the

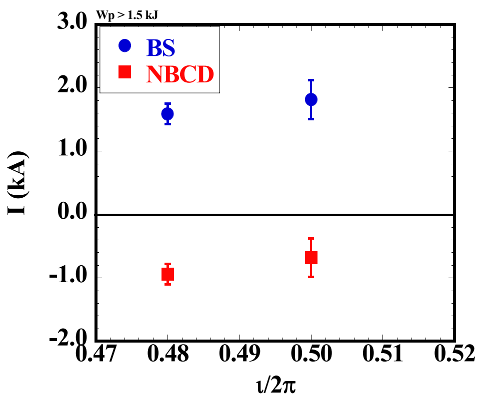

Fig. 2 Estimated bootstrap current and NB current.

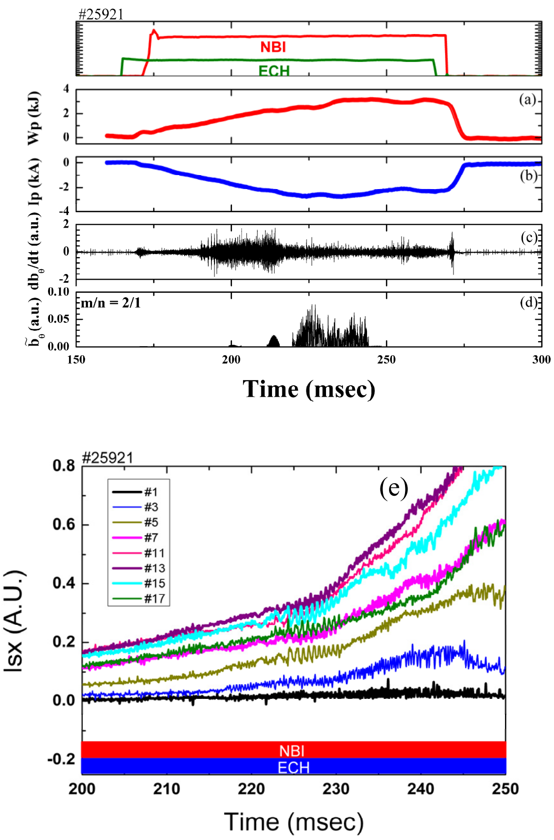

Fig. 3 Time evolution of an ECH + co- NBI plasma. The (a) stored energy, (b) toroidal current, (c) magnetic fluctuation, amplitude of (d) $m/n = 2/1$ and (e) extended view from 200 msec to 250 msec of SX signals.

NB current is -1.0 ± 0.2 kA at ι/2π= 0.48 case and -0.8 ± 0.3 kA at ι/2π = 0.50 case.

3.2 ECH + co-NBI plasma

Figure 3 shows a discharge with ECH + co-NBI at ι/2π = 0.48 configuration. The ECH power of 208 kW is injected from 165 msec to 265 msec. The NB port-through power of 573 kW is injected in the co-direction from 175 msec to 265 msec into the target plasma. The net toroidal current is increased up to 2.5 kA. The m/n = 2/1 mode with low frequency (3 kHz) is observed from 225 msec to 245 msec. The m/n =2/1 mode rotates in the electron diamagnetic direction. The SX signal synchronizes with the magnetic fluctuations with the low frequency. Figure 4(a) shows the relative amplitude of the fluctuations observed in the SX signal. The peaks are observed at 5 ch (ρ = 0.90), 15ch (ρ = 0.45) and 18ch (ρ = 0.80). Figure 4(b) shows the phase difference among SX channels for the mode. The derived phase relation indicates the 'even' or 'odd' character of the m number, that is, the phase difference between the SX channels is ~ 2π (~π) for an even (odd) m number. The phases of 5ch and 18ch are almost same and it is consistent with the m = 2 determined using the magnetic probe arrays. Therefore, they correspond to the location of the resonant surface of the m/n =2/1 mode. In vacuum magnetic surface of ι/2π = 0.48 configuration, there is no rational surface of the m/n = 2/1, however, the rotational transform is affected by the plasma pressure and co-flowing toroidal current, resulting in crossing the rational surface of the m/n = 2/1. In order to clarify the effect of the toroidal current on the equilibrium, fixed boundary VMEC calculations considering toroidal current were carried out [10]. We assume that bootstrap current density is given by $j = j_0(s\text{-}s^2)$, and NB current is given by $j = j_0(1\text{-}s)^2$, where s denotes the normalized toroidal flux, and the relationship of $s = \rho^2$ holds. The total amount of these toroidal currents was chosen to be consistent with the experimental value evaluated in Fig. 2. The electron density is given by $n_e = 2\times10^{19}(1\text{-}s^3)$ m^{-3}, and electron and ion temperature are given by $T_e = 0.45\times (1\text{-}s)^2$ keV and $T_i = 0.15\times (1\text{-}s)^2$ keV. Figure 5 shows the radial profile of the rotational transform calculated by VMEC code with toroidal current. When the bootstrap current of 1.5 kA and NB current of 1 kA flow in co-direction, the rotational transform profile has the rational surface of the m/n =2/1 around ρ = 0.8. The location of the rational surface of the m/n =2/1 calculated is consistent with that obtained by SX signals. The m/n = 2/1 mode is not observed after 245 msec. The rational surface of the m/n =2/1 may disappear by the decrease of rotational transform due to the decrease of the toroidal current.

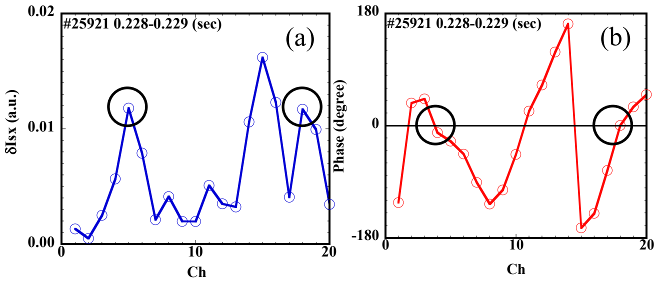

Fig. 4 Radial profile of (a) SX fluctuation amplitude and (b) phase difference among SX channels.

3.3 ECH + counter-NBI plasma

Figure 6 shows a discharge in ECH + counter-NBI with ι/2π = 0.50 configuration. The ECH pulse with the power of 312 kW is injected from 165 msec to 290 msec. The NB with the port-through power of 561 kW is injected in the counter-direction from 170 msec to 290 msec. The net toroidal current is increased up to 1 kA. The total toroidal current during counter-NBI injection is smaller than that during co-NBI injection, since the NB current flows in counter-direction against the bootstrap current. The m/n = 2/1 mode with low frequency (5 kHz) is observed from 165 msec to 280 msec. The mode rotates in electron diamagnetic direction. The SX signal synchronizing with the magnetic fluctuations of low frequency is observed. Figure 7 shows the relative amplitude of the fluctuations observed in the SX signal at 280 msec when the m/n = 2/1 mode is strongest. The peak

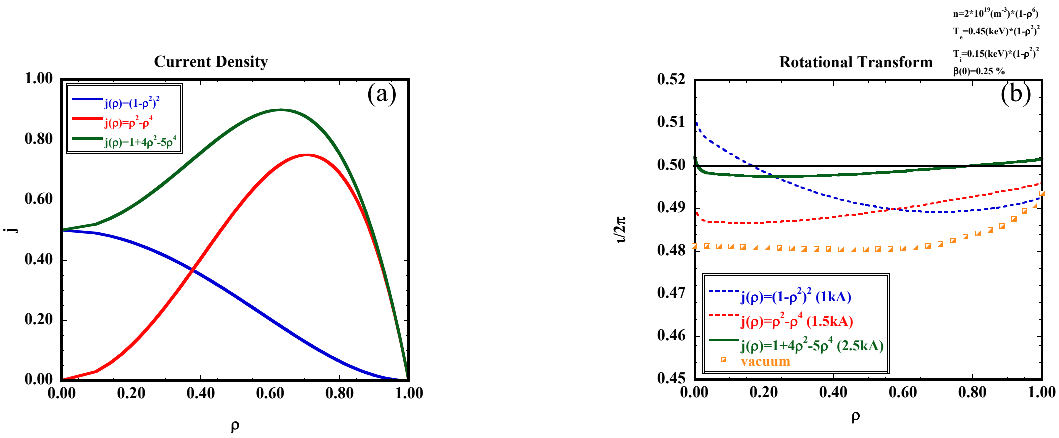

Fig. 5 (a) Toroidal current profile and (b) radial profile of rotational transform deduced from VMEC calculation with the effect of toroidal current and plasma pressure.

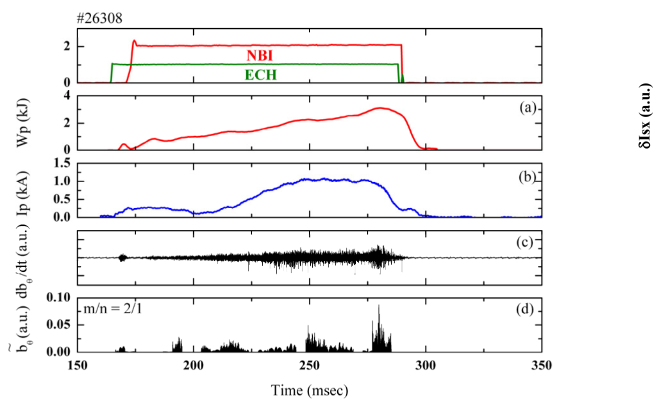

Fig. 6 Time evolution of an ECH + counter-NBI plasma. The (a) stored energy, (b) toroidal current, (c) magnetic fluctuation and amplitude of (d) m/n = 2/1.

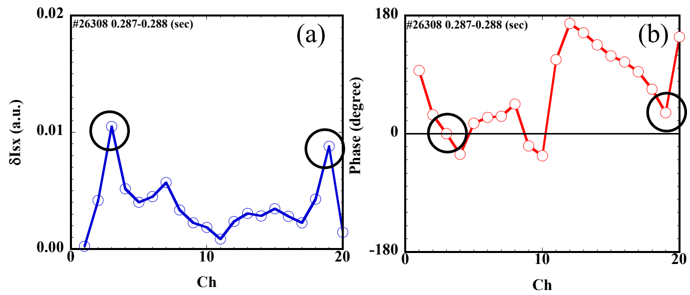

Fig. 7 Radial profile of (a) SX fluctuation amplitude and (b) phase difference among SX channels.

is observed at 3 ch and 19 ch. The phases of 3ch and 19ch are almost same and it is consistent with the m = 2 identified by magnetic probes. The positions are almost similar to the rational surface of 0.5 in vacuum condition. The VMEC calculations were performed in the same way as in the previous section. The profiles of toroidal currents and plasma pressure were similar to that of Sec 3.2. Figure 8 shows the calculated rotational transform profile with toroidal current. There is no significant difference between the rotational transform profile considering the toroidal currents and that of vacuum condition, compared with ECH + co-NBI plasma. These results suggest that the change in rotational transform profile by toroidal current is weak due to the balance between the bootstrap current and counter-flowing NB current.

4. Conclusion

The effect of toroidal current on the rotational transform has been studied in Heliotron J by measuring MHD activities. In ECH + co-NBI plasma with $\iota/2\pi$ = 0.48 configuration, the m/n = 2/1 mode with low frequency was observed when the co-flowing toroidal current is increased up to 2.5 kA. The rotational transform is probably increased by the toroidal current, resulting in crossing the rational surface. Measurement of the mode structure using a 20 channel SX detector array showed that the rational surface was located around ρ = 0.8-0.9. The increase of the rotational transform by the toroidal current is consistent with the equilibrium calculation.

The m/n = 2/1 mode was observed also in ECH + counter-NBI plasma with $\iota/2\pi$ = 0.50 configuration. By SX measurement, the rational surface was determined at the position which is not changed from that of vacuum condition. Equilibrium calculation also shows that there is no significant change in the rotational transform profile by the toroidal current. These results suggest that the change in the rotational transform profile by the toroidal current is weak in ECH + counter-NBI plasma due to the balance between bootstrap current and counter-flowing NB current.

References

[1] T. Obiki, et al., 2001 Nuclear Fusion **17** 611

[2] S. Yamamoto, et al., 2007 Fusion Sci. Technol. **51** 92

[3] G. Motojima, et al., 2007 Nuclear Fusion **47** 1045

[4] G. Motojima, et al., 2007 Fusion Sci. Technol. **51** 122

[5] S. Sakakibara, et al., 1995 Jpn. J. Appl. Phys. **34** L252

[6] E. Sallander, et al., 2000 Nuclear Fusion **40** 1499

[7] S. Kobayashi, et al., Proc. 34th EPS Conf. , Warsaw, Poland, 2007

[8] Hirshman S.P. and Betancourt O. 1991 J. Comput. Phys. **96**, 99

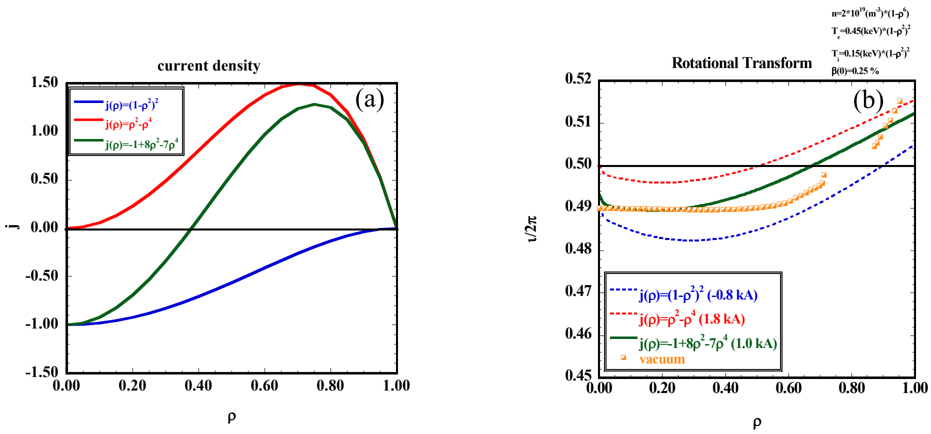

Fig. 8 (a) Toroidal current profile and (b) Radial profile of rotational transform deduced from VMEC calculation with the effect of toroidal current and plasma pressure.